Ammonia Combustion for Gas Turbine Engine Applications

Clinton Bedick [a], Andrew Tulgestke [a], Peter Strakey [b]

[a] *National Energy Technology Laboratory, Pittsburgh, PA, 15236*

[b] *National Energy Technology Laboratory, Morgantown, WV, 26505*

Abstract

The use of ammonia as a fuel source in gas turbine engine power cycles represents an attractive means to decarbonize the energy sector due to higher energy density and achieving liquid state at far lower pressures compared to pure hydrogen. However, due to low flammability and a propensity for high NOx emissions, its use is not without challenge. A number of 0D and 1D modeling tools were utilized to study the combustion characteristics of ammonia and ammonia/hydrogen mixtures, examining basic fundamental properties such as laminar flame speed, variability among existing chemical kinetic mechanisms, and considering the use of two-stage rich-lean combustion strategies to achieve low NOx emissions. This configuration showed promise for ~20 ppm NOx levels (dry, 15% O_2), however is still not optimized. Results indicate a major need for high-quality experimental validation data, in particular for quantitative species concentrations (NOx species especially). The authors are currently undertaking an experimental campaign to generate high-quality validation data sets using a flat flame burner configuration.

Introduction

The United States has set a goal of achieving net-zero greenhouse gas emissions by 2050 in order to combat the effects of climate change and limit global temperature rise to less than 1.5 C [1]. To achieve this, significant changes will be needed to the energy, transportation, and industrial sectors, all of which currently rely on carbon-based fossil fuels. Renewables such as wind and solar will play a significant role in this effort, however, combustion technologies will remain prevalent as efficient chemical energy storage and/or in applications where electrification is infeasible or impractical (ex. aero-propulsion) [1]. In these applications, the replacement of fossil-based fuels with carbon-free alternatives such as hydrogen will be required to meet decarbonization objectives in the coming years.

Over the past several decades, a great deal of progress has been made in developing hydrogen combustion technologies, including reciprocating engines [2] and gas turbines [3]. While the combustion fundamentals are feasible, a major challenge continues to be storage and transport, as the low volumetric and gravimetric density of hydrogen necessitates high-pressures (700 bar) or cryogenic temperatures (-252.8 C) to achieve liquid state [4]. Additionally, the high reactivity of hydrogen poses an increased safety risk and can result in operational challenges such as flashback and thermoacoustic instabilities [5]. Because of this, state-of-the-art gas turbine engines designed for natural gas are currently only rated for some fraction of hydrogen blending (ex. 20% - GE [6] and Siemens H-class [7]). While there is a great deal of ongoing research in transitioning these systems to 100% hydrogen [6,7], storage and transport issues have led to the consideration of other carbon-free fuels, in particular ammonia.

Ammonia (NH_3) has been proposed as an alternative carbon-free fuel source for power and propulsion applications, driven by its favorable energy density and low storage pressures, relative to hydrogen [8]. This fact could enable existing energy infrastructure (pipelines, trucks, storage tanks, etc.) to be utilized

and requires substantially less energy to compress compared to hydrogen. However, its implementation is not without challenge – in particular due to low flammability and a propensity for high nitrogen oxide (NOx) emissions [8]. Ammonia was first considered as a fuel in gas turbine engines as far back as the 1960's [9,10]. These early feasibility tests focused on the use of ammonia gas/vapor as an alternative fuel in defense applications. Here, a major finding was that combustor scale significantly influenced operability, primarily driven by the slow kinetics of ammonia-air combustion. Smaller diameter combustors and/or higher flow rates improved mixing performance but reduced residence time, leading to poor combustion efficiency or blowout. In recent years, interest in ammonia has focused on its use as a hydrogen carrier in energy applications, industry, and the potential for a liquid-based carbon-free fuel in shipping , transportation and propulsion (aero-derivative turbines) [11].

Traditionally, ammonia is produced through the Haber-Bosch process, which combines hydrogen and nitrogen over an iron-based catalyst at high temperature and pressure [8]. Production of the hydrogen feedstock can generally be considered grey, blue, or green, corresponding to utilization of fossil fuels, utilization of fossil fuels with carbon capture (typically natural gas), or through electrolysis in conjunction with electricity generated from renewables, respectively [12]. This allows hydrogen and/or ammonia production to evolve with technology and CO_2 reduction goals. Currently, there is a thriving ammonia industry, primarily associated with fertilizer production for agricultural applications [13]. Because the Haber-Bosch process is inherently inefficient and can emit considerable amounts of CO_2, there is a great deal of ongoing research in developing sustainable synthesis processes (ex. electrochemical, non-thermal plasma [13]).

Modeling tools and chemical kinetic mechanisms currently exist for simulating ammonia combustion [14–17], however they are far less developed compared to natural gas [18,19] or hydrogen [20] systems. As a result, a high degree of variability still exists in fundamental predictions of laminar flame speed and emissions characteristics [21–23]. As will be discussed below, a major finding in these works has been that lean equivalence ratios result in extremely high NOx levels due to the fuel-N, while rich equivalence ratios can mitigate this, albeit at the expense of combustion efficiency (unburnt NH_3 and/or H_2) [24–26].

Burner and combustor designs of practical interest have also been studied and characterized, both numerically, via high-fidelity CFD, and computationally. In most cases, this consists of model validation combustors with swirl stabilization [27], or in highly-strained jet flames [28], similar to what might be implemented for natural gas. There are a few examples of novel combustor designs – in particular the two-stage rich-lean concept – which show promise for good stability and low NOx emissions [26,29,30]. A similar configuration was used by Japanese researchers to demonstrate a small-scale (50 kW) ammonia-fueled gas turbine engine cycle with selective-catalytic-reduction (SCR) aftertreatment [31].

However, there are still a number of fundamental challenges which must be overcome before widespread utilization of ammonia in combustion systems can occur. As mentioned above, these challenges are primarily related to low flammability and high NOx emissions. This paper will examine these challenges, through the use of a number of currently available modeling tools and will close by presenting some preliminary results from a newly constructed ammonia combustion experiment at NETL.

Combustion Characteristics of Ammonia

The most immediate issue with ammonia as a fuel in gas turbine engines is low flammability. Typically, natural gas combustors implement high mass throughput and a compact combustor geometry to

maximize efficiency. In these systems, if natural gas were simply replaced by ammonia, the flame would likely blow off. This is because the flame speed of ammonia is drastically lower than nearly any other conventional fuel (ex. nominally: CH_4 ~ 0.37 m/s, H_2~ 2.91 m/s, NH_3 ~ 0.07 m/s [8]). Laminar flame speed, or burning velocity, represents a fundamental property defining the rate of progression of the reaction front through a uniform fuel/oxidizer mixture, at a specified temperature and pressure. Flame speed can be similarly related to the ignition delay time, the time between when the mixture is exposed to a high temperature and/or pressure condition and when exothermic heat release begins. Both of these metrics are dictated by the chemical kinetics of the combustion process.

In Fig. 1, the laminar flame speeds are plotted for CH_4, and NH_3 with varying amounts of H2 addition (0-50%). Note that here, ⅓ mole of N_2 accompanies each mole of H_2 added to the mixture, in order to simulate decomposed NH_3. Calculations were performed using a Cantera freely-propagating flame model [32], in conjunction with the well-known GRI3.0 reaction mechanism [19] for the CH4 case, and a relatively new (2017) mechanism proposed by Otomo et al. for the NH_3/H_2 cases [15].

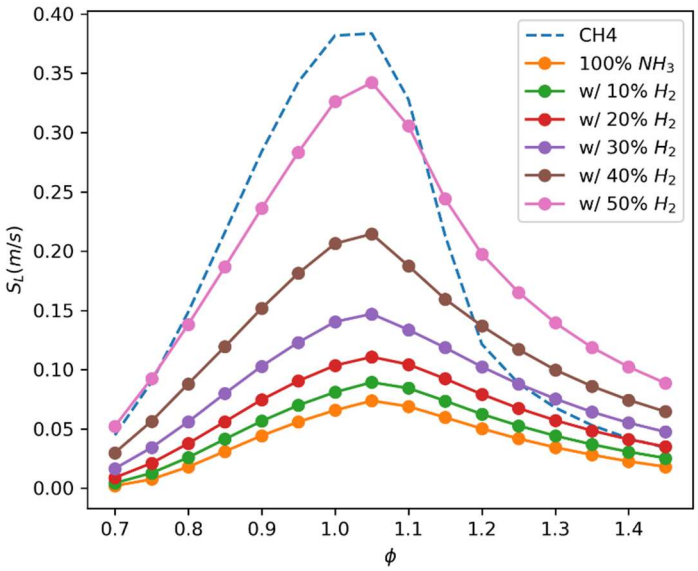

Figure 1. Laminar flame speed from Cantera freely-propagating flame model, CH_4 (GRI3.0), NH_3/H_2 mixes (Otomo et al. [15])

For all fuels, flame speed depends strongly on equivalence ratio of the mixture, reaching a maximum just above stoichiometric. Of particular interest, is the fact that ~50% H2 addition results in a flame speed very near that of methane for lean and stoichiometric equivalence ratios. For rich equivalence ratios, many of the NH_3 mixtures exceed the flame speed of CH_4, although these are conditions not often considered for hydrocarbon combustion in gas turbine engines. The main takeaway from Fig. 1, is the fact that pure NH_3/air mixtures have flame speeds nearly an order of magnitude lower than CH_4, making direct applicability in combustors designed for natural gas unlikely. Considerable stability enhancement is likely needed, via H_2 addition (NH_3 decomposition or direct H_2 synthesis through electrolysis) and/or redesign of combustor components to limit gas velocities which might otherwise blow off NH_3 flames.

Figure 2 shows an example of the species profiles from the one-dimensional Cantera freely-propagating flame model, at lean (Φ=0.7) and rich (Φ=1.4) conditions. The most immediately apparent difference is the much higher post-flame NO concentrations for the lean case, while the rich case only produces high NO within the reaction zone. Unsurprising, the lean case consumes all of the NH_3 fuel, while the rich case does not, however under rich conditions a significant amount of unburnt H_2 also remains. These trends will be further examined over a wider range of conditions in subsequent sections. Note that because these are freely-propagating flame simulations, the grid size is automatically adjusted depending on the length/time needed to achieve equilibrium conditions.

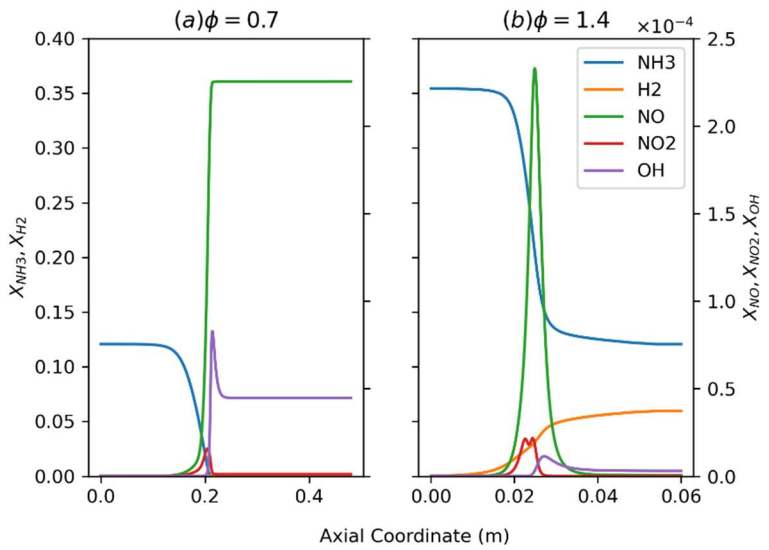

Figure 2. Species profiles from Cantera freely-propagating flame model, under lean (Φ=0.7) and rich (Φ=1.4) conditions (Otomo et al. [15])

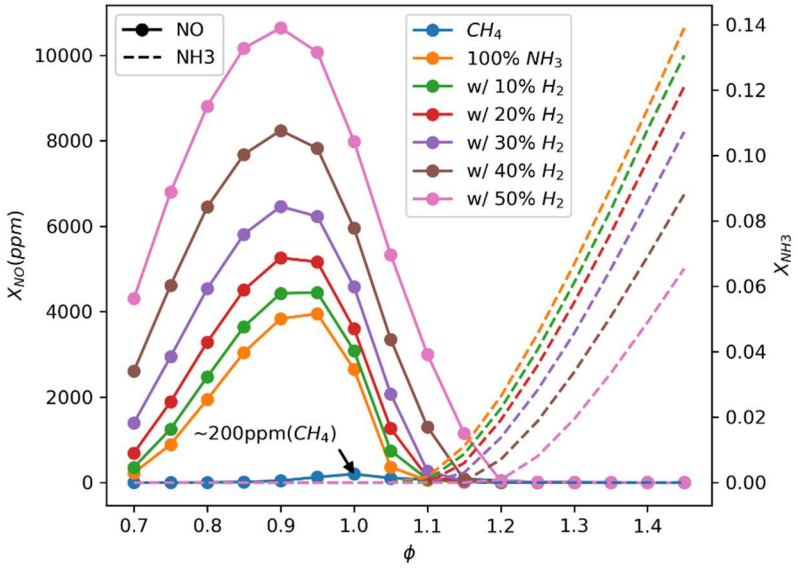

Figure 3. NO, NH_3 concentrations from Cantera freely-propagating flame model, 40 mm downstream of reaction zone, CH_4 (GRI3.0), NH_3/H_2 mixes (Otomo et al. [15])

Figure 3 shows the NO concentration 40 mm downstream of the flame front at each point in Fig. 1, along with the corresponding NH_3 concentration (dashed lines). Similar to Fig. 2, lean equivalence ratios result in extremely high NO concentrations for all NH_3 cases – in particular for those including H_2. These cases tend to have marginally elevated gas temperatures ~2000-2200 K for 100% NH_3 to 50% H_2 in NH_3), which could further accelerate NOx chemistry via enhanced radical production. The NH_3 cases see peak NO at an equivalence ratio of ~0.9, compared the CH4 flame, which reaches a maximum at stoichiometric. Immediately obvious, is the much lower NO concentration achieved by the CH4 case, primarily created through the traditional thermal-NOx routes (more on this below). Moving toward rich equivalence ratios results in a drastic reduction of NO, along with a corresponding increase in NH_3 due to lack of O_2 for complete oxidation. For the 100% NH_3 case, a happy medium may be achieved near ~Φ=1.1 for this ideal case. Increasing hydrogen content moves this optimal point toward higher equivalence ratios. While this simplified model does not tell the whole story, it provides a general understanding of the tradeoffs between NOx emissions and unburnt ammonia, supporting a two-stage combustion strategy, discussed below.

While it has been shown that GRI3.0 can be reasonably applied to ammonia systems [24], in recent years there have been a number of newly developed mechanisms specifically aimed at ammonia [14–17,33–37], which demonstrate improved predictive accuracy relative to experimental laminar flame speed and/or ignition delay time data. It should be noted that the list of mechanisms here is not exhaustive and

is largely dependent on 1) public availability of Chemkin-format reaction, thermodynamic, and transport data files, and 2) inclusion by the authors of some degree of validation against experimental data.

As with other combustion applications, mechanisms can generally be separated to consider detailed chemistry or using a reduced set of species and reactions for applicability in high fidelity CFD or other computationally intensive models. In the subset of mechanisms considered here, those from Tian [14], Konnov (2009 and full 2019 version) [17,38], Okafor [39], Glarborg [40], and Shrestha [41] might be considered 'large', with ~100+ species and 700+ reactions, while those from Stagni [42], Song [16], Otomo [15], and reduced versions of Konnov (2019) [17] might be considered 'small', with ~30 species and ~200 reactions. For modeling ammonia, a second distinction can be made between mechanisms suitable for modeling CH_4/NH_3 mixtures (i.e., includes carbon species) or not (H_2/NH_3 only). In the case of the latter, a considerable reduction of species and reactions may be possible. All of the 'large' mechanisms referenced above include carbon species, while all of the 'small' mechanisms do not. Table 1 provides a summary of the reaction mechanisms considered thus far, including the year and publication, number of species and reactions, as well as whether or not carbon compounds are considered (ex. CH_4).

In many cases, the mechanisms in Table 1 re-use portions of existing mechansms, refined as needed based on experimental observations. For example, Okafor [39] utilized carbon chemistry from GRI30 and nitrogen chemistry from Tian (2009) [14], Song [16] was largely based on prior work from Glarborg (2004, 2008, 2011), in a reduced form, Otomo [15] is a further reduction/revision to the mechanism by Song, and Konnov [17,35] utilizes H2-CH4 chemistry from AramcoMech2.0 [43]. Other mechanisms (ex. Glarborg) are based on years of revisions and evolution of chemical kinetics from experience with other fuels such as CH_4, H_2, and syngas, as well as direct validation by the authors and other independent comparisons in literature.

Table 1. Available NH_3 Combustion Reaction Mechanisms

Mech	Year	Species	Reactions	w/ C	Ref
GRI30	1999	53	325	X	[19]
Tian	2009	84	703	X	[14]
Konnov	2009	127	1207	X	[38]
Song	2016	33	204		[16]
Okafor	2018	59	356	X	[39]
Otomo	2018	32	213		[15]
Glarborg	2018	151	1397	X	[40]
Shrestha	2018	125	1089	X	[41]
Konnov	2019	28	213		[17]
		34	252		
		51	420	X	
		74	634	X	
		128	957	X	
Stagni	2020	31	203		[42]

Figure 4 shows a comparison of the predicted laminar flame speed for the same adiabatic flame simulation used in Fig. 1, for all mechanisms in Table 1. Here only a 100% ammonia case was considered. It can be immediately seen that the Konnov (2009) [38] mechanism considerably over-predicts flame speed relative

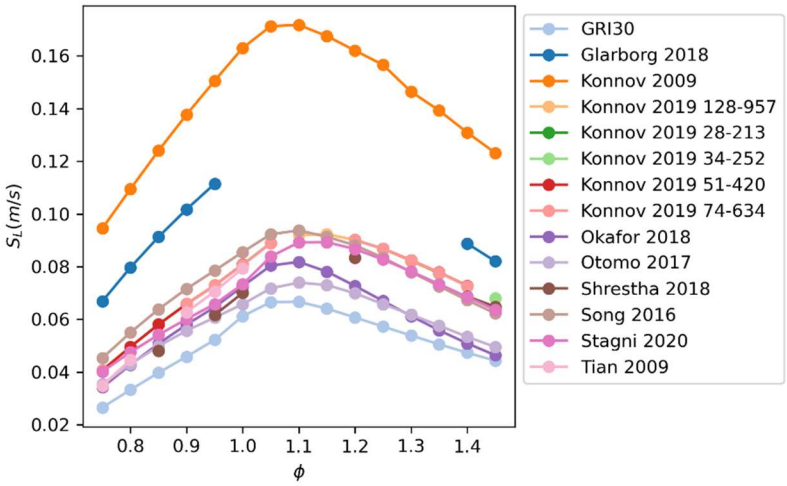

Figure 4. Chemical kinetic mechanism comparison (Table 1), laminar flame speed, Cantera freely-propagating flame simulation, 100% NH_3, 300 K, 1 atm

to the bulk grouping, as well as that of Glarborg [40]. It should also be pointed out that the Glarborg mechanism had convergence issues in the Cantera 1D flame simulation, presumably due to the large number of stiff reactions. While solver settings could likely have been adjusted to achieve convergence, most of the other mechanisms did not require this. The Tian mechanism experienced similar issues, however not as severe.

GRI3.0 under-predicted flame speed relative to the bulk grouping, but only slightly. The main takeaway from Fig. 4 is the amount of spread among these well-regarded mechanisms, amounting to nearly 30%, if disregarding Konnov (2009) [38] and Glarborg [40]. Additional comparisons should be performed at other conditions but could not be done in time for this paper.

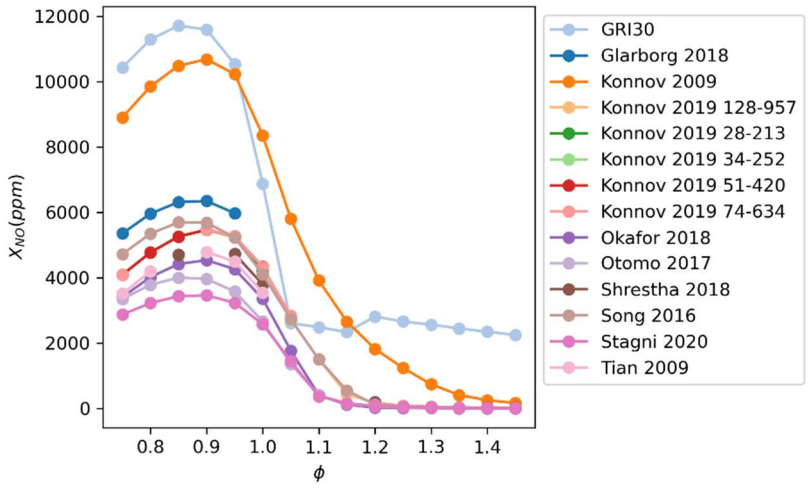

Figure 5. Chemical kinetic mechanism comparison (Table 1), NO mole fraction 40 mm downstream of reaction front, Cantera freely-propagating flame simulation, 100% NH_3, 300 K, 1 atm

Figure 5 shows the NO concentrations corresponding to the Fig. 4 data, 40 mm downstream of the reaction zone (same as Fig. 3). Under lean conditions, significant variability is seen, with GRI30 over-predicting by a factor of ~2 relative to the bulk grouping, along with Konnov (2009) [38]. The remaining mechanisms vary by ~50% under lean conditions, with slightly tighter spacing at stoichiometric and slightly rich conditions and overlapping above Φ=1.1. Note that at these rich equivalence ratios, there is still variability among mechanisms, however the NO concentrations are small such that it is of less concern.

NOx Kinetics

NOx production pathways that occur during ammonia combustion differ significantly from those during methane combustion. During natural gas combustion, the nitrogen which ends up in NOx originates from the atmosphere. High temperatures experienced during combustion thermally decompose the N_2 in the air which then reacts to form NO. In contrast, during ammonia combustion, the nitrogen which ends up in NOx primarily originates from the fuel. The pathway from NH_3 to NO can vary depending on the thermodynamic condition. Figure 6 details the NOx formation pathways during lean combustion of methane in a perfectly stirred reactor (psr) simulated using the Konnov (2019) [17] mechanism with 128 species and 957 reactions. Figure 7 shows the same condition, for ammonia. As mentioned, the nitrogen pathways and sources differ significantly, as does the complexity of the mechanism.

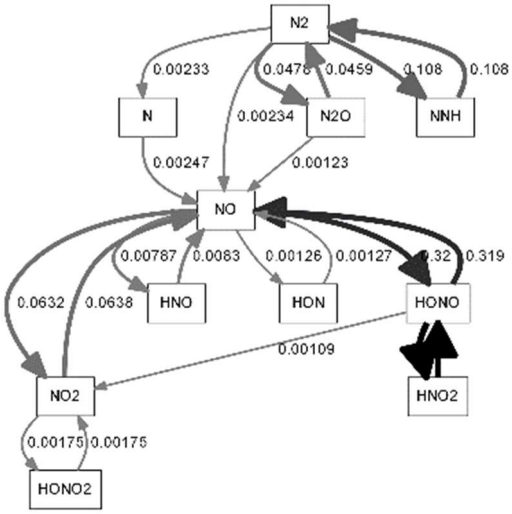

Figure 6. PSR NOx pathways, CH_4, phi=0.7, τ=3ms, 12atm, 600K preheat, Konnov 2019 [17] (128-957)

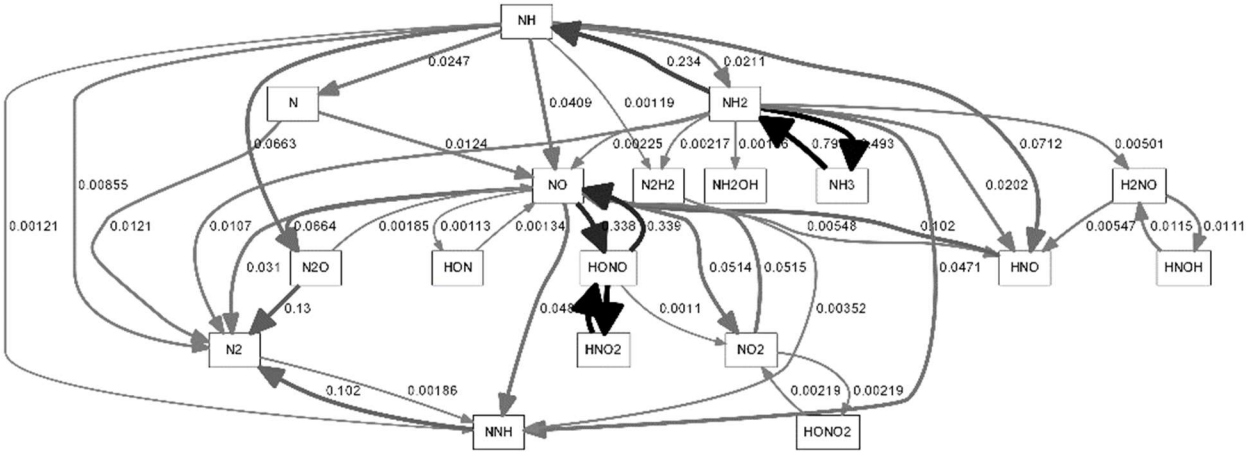

Figure 7. PSR NOx pathways, NH_3, phi=0.7, τ=3ms, 12atm, 600K preheat, Konnov 2019 [17] (128-957)

The NOx formation pathways during rich ammonia combustion are largely the same as those during lean combustion. However, less NOx is formed during rich combustion due to the lack of available oxygen atoms. For a single stage reactor consisting of a PSR followed by a plug flow reactor (PFR) at the condition of Fig. 7, (phi=0.7), the NOx level corrected to 15 % O_2 was 1686 ppm. At a rich condition of phi=1.3, the

NOx drops to 18 ppm, or 17 ppm when 15 percent-by-volume of the fuel is replaced by H_2. This drastic decrease in NOx production shows a possible way forward with ammonia as a fuel source if the remaining unburnt fuel can be cleanly oxidized. This line of thought has led to interest in a multi-staged combustion approach for ammonia fuels.

In a multi-stage combustor, some additional NOx may be generated in the later stages as the unburnt fuel is consumed. However, the NOx level remains much lower than what would result from a single stage combustor. The reaction pathway for the 2nd stage of a 2-stage ammonia combustor shown in Fig. 8, having a rich first stage of phi=1.3 followed by a lean second stage for a global phi of 0.7, shows that NO reactions are primarily interconversion reactions between other small radicals. Formation of new NO from fuel or air is comparatively insignificant, being less than 1000 times smaller than the NO flux from interconversion reactions. This occurs as the unburnt fuel is being oxidized. The NOx level again corrected to 15 % O_2 following the second stage reactor has only slightly increased to 39 ppm, or 48 ppm when 15 percent-by-volume of the fuel is replaced by H_2.

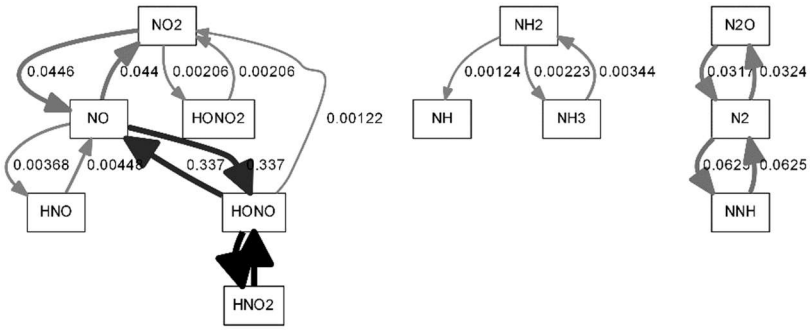

Figure 8. PSR (second stage) NOx pathways, Φ_g =0.7, Φ_r =1.3, τ=2ms, 12atm, 600K preheat, Konnov 2019 [17] (128-957)

Novel Combustion Strategies

While challenges related to the low flammability of ammonia remain, these issues are more readily solvable through combustor design and/or upstream reforming such that an operable ammonia-fueled gas turbine engine seems feasible. This has in fact been demonstrated, albeit at reduced scale, more than 50 years ago [9,10]. The more pressing issue related to ammonia combustion is undoubtedly the NOx emissions. If not solvable, this has the potential to be a showstopper for the technology in general. It has been proposed by a number of researchers [8,26,29,31,44] that a two-stage rich-lean combustion strategy has the potential for achieving low NOx emissions. This approach essentially converts a fraction of the NH_3 to H_2 through oxidation, while limiting O_2 availability for formation of large amounts of O and OH radicals. As shown in the previous section, these radicals are crucial to many of the NOx formation pathways. It should also be noted that this process differs from thermal decomposition of NH_3 to H_2 and N_2, in that it is exothermic, thus contributing to the thermal input to the turbine.

At some downstream location, secondary air is injected into the combustor, quenching the rich flame and providing a lean burn environment in which remaining NH_3 and H_2 fuel burnout occurs. Ideally, most of the NH_3 has been consumed or converted to H_2 the rich stage, such that NOx formation in the lean stage is via the more traditional thermal route, which may be mitigated by maintaining cool flame temperatures. Additionally, it would be hoped that any NOx formed in the rich stage is converted to N_2 from the

quenching process. In reality however, there is expected to be some amount of un-decomposed NH_3 that makes its way from the rich to the lean stage, as a result of finite residence times afforded by combustor geometry. Similarly, tradeoffs between the quenching effect of secondary air injection and a potential for high NOx emissions from un-decomposed NH_3 at very lean conditions must be considered.

Prior to performing computationally intensive 2D or 3D CFD, a chemical-reactor-network (CRN) model is particularly useful for two-stage rich-lean combustion strategies. This has been studied by a number of researchers [26,45–47]. A particular finding of these works was the significance of the rich stage equivalence ratio and residence time on the overall NOx emissions. To consider these effects, a CRN was developed using Cantera, in a similar manner to Refs [26,45–47]. Here, each stage of the two-stage combustor was represented as a perfectly-stirred-reactor (PSR), meant to represent the recirculating flame zone, followed by a plug-flow-reactor (PFR), meant to represent the post flame zone. Chemical kinetics were integrated within each reactor, and the residence times were specified for each. For the PSR, because Cantera does not allow the residence time to be explicitly set, the reactor volume was adjusted iteratively using a specified total mass flow rate, until the desired residence time was achieved.

Upstream of the rich-stage PSR-PFR network, a premixed air/fuel composition was specified. The rich stage exit state was passed on to the lean stage, along with some amount of secondary air injection. Here, the secondary air mass flow rate was computed according to a desired global equivalence ratio for the two-stage system, as shown in Eq. 1. Here, $FAR_{\Phi=1}$ is the stoichiometric fuel-air-ratio (FAR) on a mass-basis, and Φ_r and $\dot{m}_1$ are the rich stage equivalence ratio and rich stage total mass flow rate (air + fuel), respectively.

$$\dot{m}_{air-2} = \dot{m}_1 \left[\frac{\left(1 - \frac{1}{\Phi_r \cdot FAR_{\Phi=1}}\right)}{\Phi_g \cdot FAR_{\Phi=1}} - \frac{1}{\Phi_r \cdot FAR_{\Phi=1}} \right] \quad \text{Eq. (1)}$$

Ultimately the mass flow rates specified are irrelevant, as the residence times are explicitly defined in the simulation, however they are used to inform the relative mass fractions of the rich stage exit composition and secondary air. Figure 9 shows the layout of the two-stage PSR-PFR CRN model.

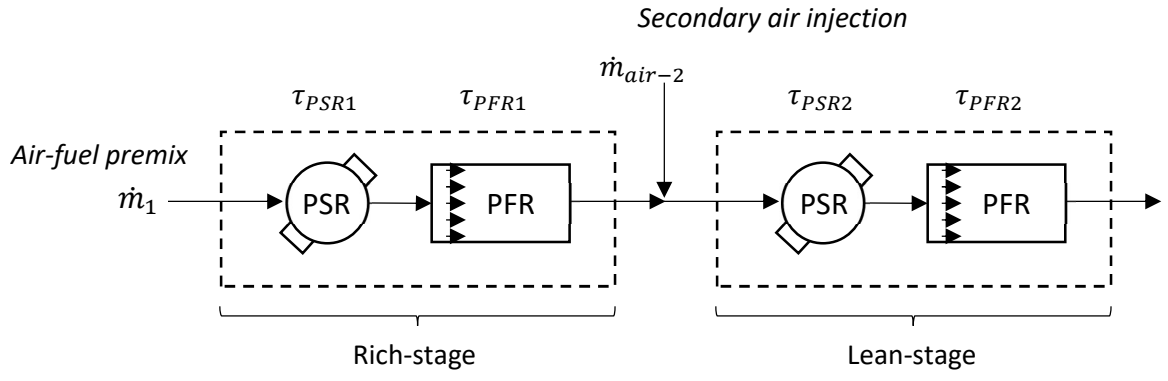

Figure 9. Two-stage rich-lean ammonia combustion model using PSR-PFR CRN

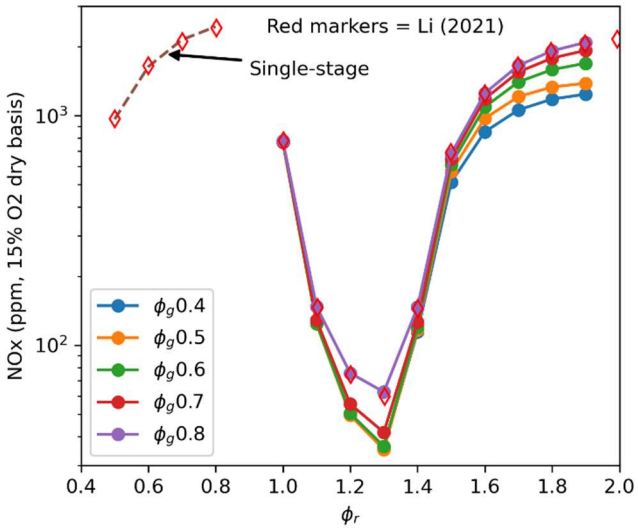

Figure 10. Cantera two-stage PSR-PFR CRN NOx (15% O2 dry), along with Chemkin results from Li et al. [26], including 15% H_2 addition, 600 K preheat, 12 atm

The resulting simulation has a great deal of variables which can be adjusted, and perhaps would make for a good optimization problem in future endeavors. As an initial test, the model was run, and the results compared to published data from Li et al. [26]. Here, a major interest was matching results produced using commercial software package Chemkin, with the open-source Cantera. While the two packages are similar, the way in which reactor volume, residence time, and mass throughput are handled differs considerably, as well as the numerical solvers used for kinetics integration. The model was run for the same conditions as Li et al. [26], which included 15% H_2 addition by volume, 12 atm pressure, 600 K preheat of the premixed reactants and secondary air injection, rich stage PSR and PFR residence times of 3 ms and 14 ms, respectively, and lean stage PSR and PFR residence times of 2 ms and 1 ms, respectively. A range of rich and global equivalence ratios were considered.

The resulting NOx emissions are shown in Fig. 10, along with those from Li et al. [26], both corrected to 15% O_2 on a dry basis. In the upper left corner, are NOx concentrations for the case of single stage lean combustion of ammonia (PSR/PFR residence times 3ms/14ms). Here, the emissions are very high due to the lean conditions, demonstrating unsuitability of a single stage lean premixed combustion strategy. Of greater interest, are the two-stage exit NOx emissions, shown as the solid lines in Fig. 10. A substantial reduction of NOx is seen near Φ~1.2-1.3, with a very steep slope on either side. With regard to model validation, both the single and two-stage rich-lean results match extremely well between the Cantera model and Chemkin model data from Li et al. [26].

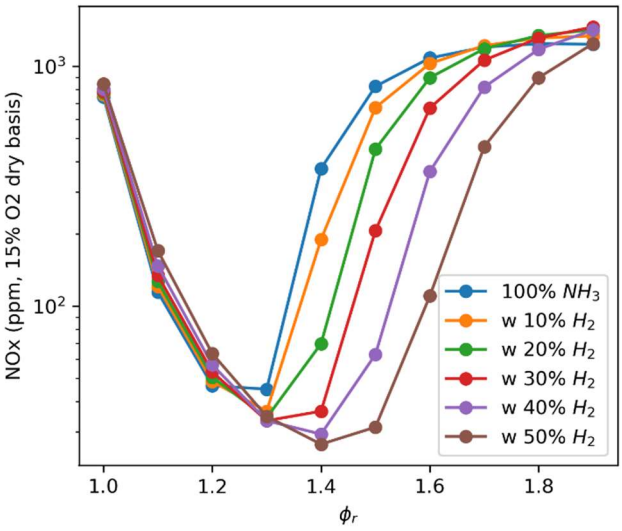

Figure 11. Cantera two-stage PSR-PFR CRN NOx for 100% NH_3 and varying amounts of H_2 addition, 600 K preheat, 12 atm

Figure 11 shows the same residence times, pressure, and preheat temperature, but with a fixed global equivalence ratio of 0.5 and varying amounts of H_2 addition (by volume). A similar trend is exhibit to Fig. 10; however, the minimum NOx point moves toward higher rich stage equivalence ratios as H_2 is added. Additionally, the low-NOx region expands, indicating some extension of operability for these higher H_2 cases. For 50% H_2 addition, the minimum NOx point is ~20 ppm.

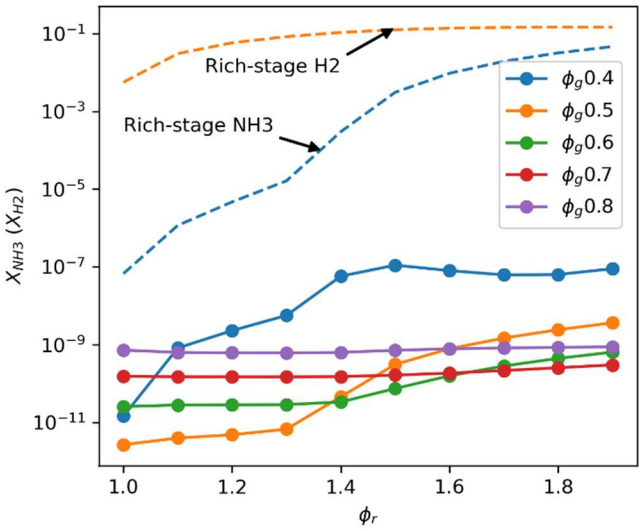

Figure 12. Cantera two-stage PSR-PFR CRN exit NH_3, rich stage NH_3, H_2

To further explore the two-stage concept, Fig. 12 shows the NH_3 emissions from the lean stage, as well as the H_2 and NH_3 emissions from the rich stage, prior to secondary air injection. Of particular interest here, is 1) the extremely low unburnt NH_3 emissions at the lean stage exit, and 2) the significant NH_3-H_2 conversion within the rich stage, while simultaneously consuming most of the available NH_3. Additionally, when considering equivalence ratio trends, it can be seen that the leanest global equivalence ratios actual result in higher lean stage exit NH_3, presumably due to limited conversion at these extremely lean conditions. It is possible here, that a stable flame may not be supported, which would need to be further confirmed via CFD. Finally, examining trends in NH_3-H_2 conversion with rich stage equivalence ratio, it can be seen that the amount of H_2 produced flattens considerably above ~Φ=1.5, suggesting equivalence ratios above this may not provide a benefit.

Next, the impact of residence time was evaluated. Conceptually, this might be separated into two considerations, 1) NH_3 to H_2 conversion in the rich stage, and 2) NOx quench and reduction in the lean stage, plus burnout of any remaining H_2 and NH_3. These processes are likely significantly affected by residence time, as it will ultimately dictate the time available for reactions to progress. The model was run at a single equivalence ratio point, Φ_r=1.3 and Φ_g=0.6, perhaps representing an optimal point on Figs. 10 and 11. In Fig. 10-12, the total rich stage residence time was 17 ms, and the ratio τ_{PSR1}/τ_{PFR1} was ~0.2.

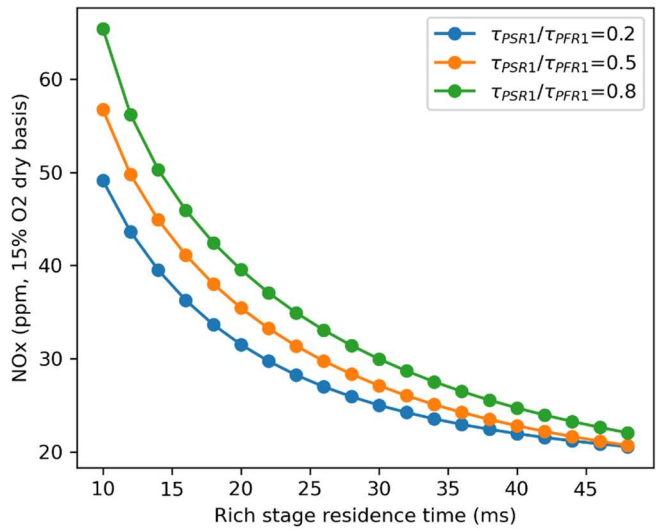

Figure 13. Cantera two-stage PSR-PFR CRN exit NOx vs. rich-stage residence time, for varying τ_{PSR1}/τ_{PFR1} ratios

In Fig. 13, the lean stage exit NOx, corrected to 15% O2 on a dry basis, is plotted as a function of the total rich stage residence time, for τ_{PSR1}/τ_{PFR1} ratios of 0.2, 0.5, and 0.8. Here, altering the ratio of PSR to PFR residence time may represent different flame shapes, with lower values indicating a compact, high-turbulence flame, and higher values indicating a long, highly strained flame. The results in Fig. 13 show that further NOx reductions are possible by extending the residence time of the rich stage, however the benefits are reduced as residence time is increased. Additionally, heat losses were not

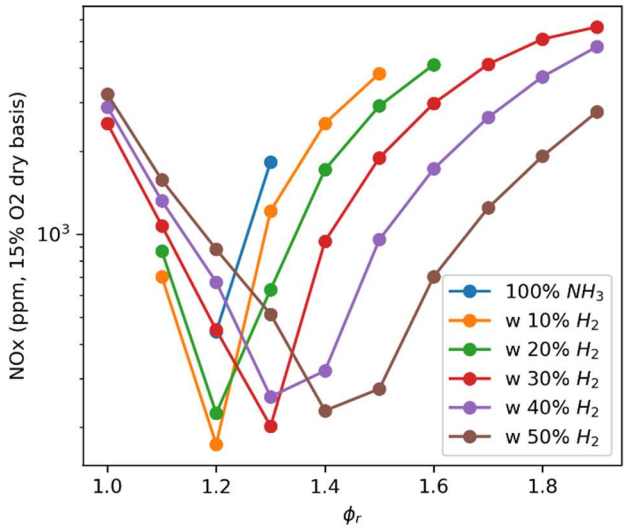

Figure 14. Cantera two-stage PSR-PFR CRN NOx for 100% NH_3 and varying amounts of H_2 addition, 300 K preheat, 1 atm

considered in this model, which could be significant as the length of the combustor is increased. Shorter flame zones are also favored due to greater interaction between hot products and cool reactants. A similar comparison was performed for the lean stage, however it resulted in < 1 ppm difference in NOx emissions over a similar parameter space.

Finally, a simple analysis was done at atmospheric pressure and 300 K inlet temperature, to investigate the impacts on operability and NOx emissions. This is of particular interest to the authors for future work in developing and testing a two-stage model validation combustor for ammonia. Figure 14 is a duplication of Fig. 11, at 300 K and 1 atm. Here, only points which ignited in the rich stage are represented. Immediately, it can be seen that the NOx levels are far higher in at 1 atm and 300 K. This is largely driven by NH_3 to H_2 conversion in the rich stage, which is much lower at reduced temperature and pressure. As a result, the lean stage combustion produces substantial NOx (ex. see single stage lean results in Fig. 10). Here, one solution could be extending the rich stage residence time, however at this reduced temperature and pressure condition, the practicality of this may be limited, especially when considering heat losses. The other takeaway from Fig. 14, is the substantially reduced operational range. For 100% NH_3, only Φ_r=1.2 and 1.3 ignited, while 10% extends this to Φ_r=1.1-1.5, and 50% H_2 allows the full equivalence ratio range. This is an important consideration for any atmospheric pressure burner tests, as limited operational conditions may be possible.

Conclusions and Future Work

In summary, the combustion characteristics of ammonia have been explored using 0D and 1D modeling tools in conjunction with Cantera. The low flammability of ammonia results in laminar flame speed which is nearly an order of magnitude lower than that of methane. As a result, direct applicability in combustors designed for natural gas may be problematic. Similar to other fuels, the flame speed peaks at an equivalence ratio of ~1.1 and converting ~50% of the NH_3 to H_2 and H_2 via thermal catalytic decomposition can approximately match the flame speed of methane. For NOx, the fuel-N is particularly problematic. Under lean conditions typical of natural gas combustion, NOx levels approach 10,000 ppm. However, under rich conditions, low NOx emissions can be achieved, albeit with poor fuel conversion (high unburnt NH_3, H_2).

A number of chemical kinetic mechanisms are currently available in the literature, in both reduced and detailed form. GRI30 includes reactions suitable for modeling NH_3, H_2, and CH_4 fuel mixes, however predictive accuracy suffers compared to more specialized offerings for NH_3. Flame speeds and NO concentrations were determined using a 1D adiabatic flame model for (14) mechanisms. A 300K and 1 atm initial condition was considered, and 100% NH_3 fuel. Flame speeds showed considerable spread, with

GRI falling lowest, and Glarborg [40] and Konnov (2009) [38] appearing highest. Most other mechanisms fell within ~30% of one another. Post-flame NO concentration variability was even higher, with Glarborg [40] and Konnov (2009) [38] being outliers and ~50% variability exhibited for lean equivalence ratios. Additionally, some of the more detailed mechsnisms (ex. Glarborg [40], Tian [14]) had difficulties converging at many conditions. While adjustments to solver settings may have enabled convergence, this was not required for most other mechanisms. This is likely important in any subsequent CFD studies.

The formation of NOx was further investigated through a basic pathway analysis using the Tian mechanism [14]. The substantial differences in nitrogen sources were highlighted relative to CH_4, and while the same pathways existed for rich and lean NH_3 combustion, oxygen availability ultimately limits NOx formation in the rich case. In all cases, NOx formation was strongly dependent on interconversion reactions between other small radicals (ex. O, OH, H). Finally, a two-stage rich-lean combustion strategy was studied using a PSR-PFR approach. First, the use of Cantera to simulate this system was validated by comparing results to those from literature [26], showing excellent agreement. Next, a number of simple parametric studies were performed to investigate the impact of equivalence ratio, hydrogen addition, residence time, and temperature and pressure. Of particular importance was rich-stage equivalence ratio, which showed a narrow range which could result in low NOx emissions. This range tended to expand with hydrogen addition and move toward higher equivalence ratios. NOx levels as low as ~20 ppm (dry, 15% O_2) could be achieved depending on conditions. The impact of temperature and pressure was also significant, such that a 1 atm, 300 K inlet temperature combustor may have limited operability, depending on H_2 addition.

While the two-stage rich-lean combustion strategy shows significant promise for low-NOx combustion of ammonia, model predictions are still lacking rigorous validation. In particular, the mechanism comparison results in Fig. 4 and 5 demonstrate nearly an order of magnitude variability. Before significant conclusions can be drawn about the viability of ammonia combustion technologies, and the development and testing of well-informed practical hardware configurations can occur, further validation is needed. In particular, detailed measurements of species concentrations associated with NOx formation. The authors are currently in the process of performing these measurements at the National Energy Technology Laboratory.

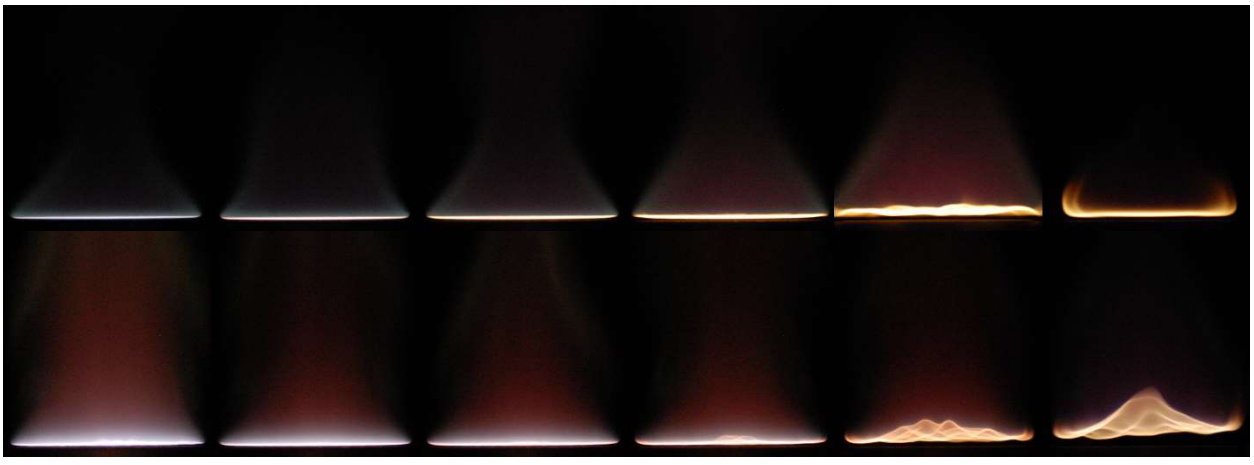

Figure 15. H_2/NH_3 (top row), CH_4/NH_3 (bottom row) flat flames, 30-80% by volume NH_3 (left to right), 5 slpm total fuel flow

While quantitative measurement data was not available in time for this paper, Fig. 15 shows an example of NH_3/H_2 (top row) and NH_3/CH_4 (bottom row) flames established using a flat-flame burner. For H_2/NH_3 mixes, the flame transitions from a nearly invisible, perfectly flat flame, to a slightly lifted, orange flame due to NH_3 emission bands. The CH_4/NH_3 mixes exhibit a thicker reaction zone as a result of the lower flame speeds, becoming cellular and unstable at ~60-70% NH_3 by volume. The H_2/NH_3 mixes do not become as wrinkled and cellular for higher NH_3 content, however the reaction zone thickens, and the edges lift as a result of heat loss to the burner and interaction with the surrounding shroud flow. Flame speed measurements are in progress using a burner heat flux method, and detailed species profiles will be determined using absorptive spectroscopic techniques (FTIR, TDLAS, hyperspectral imaging).

References

[1] The long-term strategy of the United States: pathways to net-zero greenhouse gas emissions by 2050. Washington, DC: 2021.

[2] Akal D, Öztuna S, Büyükakın MK. A review of hydrogen usage in internal combustion engines (gasoline-Lpg-diesel) from combustion performance aspect. Int J Hydrogen Energy 2020;45:35257–68. https://doi.org/10.1016/j.ijhydene.2020.02.001.

[3] Langston LS. Hydrogen Fueled Gas Turbines. Mech Eng 2019;141:52–4. https://doi.org/10.1115/1.2019-MAR-6.

[4] Hydrogen Storage. US Dep Energy n.d. https://www.energy.gov/eere/fuelcells/hydrogen-storage#:~:text=Hydrogen can be stored physically,pressure is −252.8°C.

[5] Eggenspieler G, Strakey P, Sidwell T. Experimental and Numerical Study of Flashback in the SimVal Combustion Chamber. 46th AIAA Aerosp. Sci. Meet. Exhib., Reston, Virigina: American Institute of Aeronautics and Astronautics; 2008. https://doi.org/10.2514/6.2008-1025.

[6] GE, DOE Accelerating the Path towards 100% Hydrogen Combustion in Gas Turbines. Gen Electr Press Release 2022. https://www.ge.com/news/press-releases/ge-doe-accelerating-the-path-towards-100-hydrogen-combustion-in-gas-turbines.

[7] Patel S. Siemens' Roadmap to 100% Hydrogen Gas Turbines. Power Mag 2020. https://www.powermag.com/siemens-roadmap-to-100-hydrogen-gas-turbines/.

[8] Kobayashi H, Hayakawa A, Somarathne KDKA, Okafor EC. Science and technology of ammonia combustion. Proc Combust Inst 2019;37:109–33. https://doi.org/10.1016/j.proci.2018.09.029.

[9] Solar Turbines. Development of an ammonia-burning gas turbine engine. 1966.

[10] Pratt DT. Performance of ammonia-fired gas-turbine combustors. 1967.

[11] Industry V, Innovators M, Kizer A, Butler J, Britton N, Comello S, et al. The Future of Clean Hydrogen in the United States : 2021.

[12] Tullo AH. Is ammonia the fuel of the future? Chem Eng News 2021. https://cen.acs.org/business/petrochemicals/ammonia-fuel-future/99/i8.

[13] Ghavam S, Vahdati M, Wilson IAGG, Styring P. Sustainable Ammonia Production Processes. Front Energy Res 2021;9:1–19. https://doi.org/10.3389/fenrg.2021.580808.

[14] Tian Z, Li Y, Zhang L, Glarborg P, Qi F. An experimental and kinetic modeling study of premixed

NH3/CH4/O2/Ar flames at low pressure. Combust Flame 2009;156:1413–26. https://doi.org/10.1016/j.combustflame.2009.03.005.

[15] Otomo J, Koshi M, Mitsumori T, Iwasaki H, Yamada K. Chemical kinetic modeling of ammonia oxidation with improved reaction mechanism for ammonia/air and ammonia/hydrogen/air combustion. Int J Hydrogen Energy 2018;43:3004–14. https://doi.org/10.1016/j.ijhydene.2017.12.066.

[16] Song Y, Hashemi H, Christensen JM, Zou C, Marshall P, Glarborg P. Ammonia oxidation at high pressure and intermediate temperatures. Fuel 2016;181:358–65. https://doi.org/10.1016/j.fuel.2016.04.100.

[17] Li R, Konnov AA, He G, Qin F, Zhang D. Chemical mechanism development and reduction for combustion of NH3/H2/CH4 mixtures. Fuel 2019;257:116059. https://doi.org/10.1016/j.fuel.2019.116059.

[18] Kazakov, A.; Frenklach M. Reduced reaction sets based on GRI-Mech 1.2 n.d. http://www.me.berkeley.edu/drm/.

[19] Smith GP, Golden DM, Frenklach M, Moriarty NW, Eiteneer B, Mikhail Goldenberg, C. Thomas Bowman, Ronald K. Hanson SS, et al. GRI Mech 3.0 n.d. http://www.me.berkeley.edu/gri_mech/.

[20] Li J, Zhao Z, Kazakov A, Dryer FL. An updated comprehensive kinetic model of hydrogen combustion. Int J Chem Kinet 2004;36:566–75. https://doi.org/10.1002/kin.20026.

[21] Kumar P, Meyer TR. Experimental and modeling study of chemical-kinetics mechanisms for H2–NH3–air mixtures in laminar premixed jet flames. Fuel 2013;108:166–76. https://doi.org/10.1016/j.fuel.2012.06.103.

[22] Hayakawa A, Goto T, Mimoto R, Arakawa Y, Kudo T, Kobayashi H. Laminar burning velocity and Markstein length of ammonia/air premixed flames at various pressures. Fuel 2015;159:98–106. https://doi.org/10.1016/j.fuel.2015.06.070.

[23] Li J, Lai S, Chen D, Wu R, Kobayashi N, Deng L, et al. A Review on Combustion Characteristics of Ammonia as a Carbon-Free Fuel. Front Energy Res 2021;9:1–15. https://doi.org/10.3389/fenrg.2021.760356.

[24] Han X, Wang Z, Costa M, Sun Z, He Y, Cen K. Experimental and kinetic modeling study of laminar burning velocities of NH 3 / air , NH 3 / H 2 / air , NH 3 / CO / air and NH 3 / CH 4 / air premixed flames. Combust Flame 2019;206:214–26. https://doi.org/10.1016/j.combustflame.2019.05.003.

[25] Hayakawa A, Goto T, Mimoto R, Kudo T, Kobayashi H. NO formation / reduction mechanisms of ammonia / air premixed flames at various equivalence ratios and pressures 2015;2:1–10. https://doi.org/10.1299/mej.14-00402.

[26] Li Z, Li S. Kinetics modeling of NOx emissions characteristics of a NH3/H2 fueled gas turbine combustor. Int J Hydrogen Energy 2021;46:4526–37. https://doi.org/10.1016/j.ijhydene.2020.11.024.

[27] Zhang M, An Z, Wang L, Wei X, Jianayihan B, Wang J, et al. The regulation effect of methane and hydrogen on the emission characteristics of ammonia/air combustion in a model combustor. Int J Hydrogen Energy 2021;46:21013–25. https://doi.org/10.1016/j.ijhydene.2021.03.210.

[28] Um DH, Joo JM, Lee S, Kwon OC. Combustion stability limits and NOx emissions of nonpremixed ammonia-substituted hydrogen-air flames. Int J Hydrogen Energy 2013;38:14854–65. https://doi.org/10.1016/j.ijhydene.2013.08.140.

[29] Somarathne KDKA, C. Okafor E, Hayakawa A, Kudo T, Kurata O, Iki N, et al. Emission characteristics of turbulent non-premixed ammonia/air and methane/air swirl flames through a rich-lean combustor under various wall thermal boundary conditions at high pressure. Combust Flame 2019;210:247–61. https://doi.org/10.1016/j.combustflame.2019.08.037.

[30] Somarathne KDKA, Hatakeyama S, Hayakawa A, Kobayashi H. Numerical study of a low emission gas turbine like combustor for turbulent ammonia/air premixed swirl flames with a secondary air injection at high pressure. Int J Hydrogen Energy 2017;42:27388–99. https://doi.org/10.1016/j.ijhydene.2017.09.089.

[31] Kurata O, Iki N, Inoue T, Matsunuma T, Tsujimura T, Furutani H, et al. Development of a wide range-operable, rich-lean low-NOx combustor for NH 3 fuel gas-turbine power generation. Proc Combust Inst 2019;37:4587–95. https://doi.org/10.1016/j.proci.2018.09.012.

[32] Goodwin DG, Speth RL, Moffat HK, Weber. BW. Cantera: An object-oriented software toolkit for chemical kinetics, thermodynamics, and transport processes 2018. https://doi.org/10.5281/zenodo.1174508.

[33] Okafor EC, Naito Y, Colson S, Ichikawa A, Kudo T, Hayakawa A, et al. Experimental and numerical study of the laminar burning velocity of CH4–NH3–air premixed flames. Combust Flame 2018;187:185–98. https://doi.org/10.1016/j.combustflame.2017.09.002.

[34] Stagni A, Cavallotti C, Arunthanayothin S, Song Y, Herbinet O, Battin-Leclerc F, et al. An experimental, theoretical and kinetic-modeling study of the gas-phase oxidation of ammonia. React Chem Eng 2020;5:696–711. https://doi.org/10.1039/C9RE00429G.

[35] Konnov AA. Implementation of the NCN pathway of prompt-NO formation in the detailed reaction mechanism. Combust Flame 2009;156:2093–105. https://doi.org/10.1016/j.combustflame.2009.03.016.

[36] Glarborg P, Miller JA, Ruscic B, Klippenstein SJ. Modeling nitrogen chemistry in combustion. Prog Energy Combust Sci 2018;67:31–68. https://doi.org/10.1016/j.pecs.2018.01.002.

[37] Shrestha KP, Seidel L, Zeuch T, Mauss F. Detailed Kinetic Mechanism for the Oxidation of Ammonia Including the Formation and Reduction of Nitrogen Oxides. Energy & Fuels 2018;32:10202–17. https://doi.org/10.1021/acs.energyfuels.8b01056.

[38] Konnov AA. Implementation of the NCN pathway of prompt-NO formation in the detailed reaction mechanism. Combust Flame 2009;156:2093–105. https://doi.org/10.1016/j.combustflame.2009.03.016.

[39] Okafor EC, Naito Y, Colson S, Ichikawa A, Kudo T, Hayakawa A, et al. Experimental and numerical study of the laminar burning velocity of CH4–NH3–air premixed flames. Combust Flame 2018;187:185–98. https://doi.org/10.1016/j.combustflame.2017.09.002.

[40] Glarborg P, Miller JA, Ruscic B, Klippenstein SJ. Modeling nitrogen chemistry in combustion. Prog Energy Combust Sci 2018;67:31–68. https://doi.org/10.1016/j.pecs.2018.01.002.

[41] Shrestha KP, Seidel L, Zeuch T, Mauss F. Detailed Kinetic Mechanism for the Oxidation of

Ammonia Including the Formation and Reduction of Nitrogen Oxides. Energy & Fuels 2018;32:10202–17. https://doi.org/10.1021/acs.energyfuels.8b01056.

[42] Stagni A, Cavallotti C, Arunthanayothin S, Song Y, Herbinet O, Battin-Leclerc F, et al. An experimental, theoretical and kinetic-modeling study of the gas-phase oxidation of ammonia. React Chem Eng 2020;5:696–711. https://doi.org/10.1039/C9RE00429G.

[43] Li Y, Zhou C-W, Somers KP, Zhang K, Curran HJ. The oxidation of 2-butene: A high pressure ignition delay, kinetic modeling study and reactivity comparison with isobutene and 1-butene. Proc Combust Inst 2017;36:403–11. https://doi.org/10.1016/j.proci.2016.05.052.

[44] Hayakawa A, Arakawa Y, Mimoto R, Somarathne KDKA, Kudo T, Kobayashi H. Experimental investigation of stabilization and emission characteristics of ammonia/air premixed flames in a swirl combustor. Int J Hydrogen Energy 2017;42:14010–8. https://doi.org/10.1016/j.ijhydene.2017.01.046.

[45] Li Z, Li S. Effects of inter-stage mixing on the NOx emission of staged ammonia combustion. Int J Hydrogen Energy 2022;47:9791–9. https://doi.org/10.1016/j.ijhydene.2022.01.050.

[46] Hussein NA, Valera-Medina A, Alsaegh AS. Ammonia- hydrogen combustion in a swirl burner with reduction of NOx emissions. Energy Procedia 2019;158:2305–10. https://doi.org/10.1016/j.egypro.2019.01.265.

[47] Xiao H, Valera-Medina A, Marsh R, Bowen PJ. Numerical study assessing various ammonia/methane reaction models for use under gas turbine conditions. Fuel 2017;196:344–51. https://doi.org/10.1016/j.fuel.2017.01.095.